

Kinetic Spectroscopy of Pyrazolotriazole Azomethine Dyes

Francis Wilkinson,* David Worrall, David McGarvey and Andrew Goodwin

Department of Chemistry, University of Technology, Loughborough, Leicestershire, UK LE11 3TU

Andrew Langley

Laser Support Facility, Rutherford-Appleton Laboratory, Chilton, Didcot, Oxfordshire, UK

The photophysical properties of pyrazolotriazole azomethine dyes have been investigated using both picosecond and nanosecond flash photolysis. On nanosecond timescales, prompt formation of a photoisomer is observed, the rate of decay of which shows a solvent dependence. In the presence of a triplet sensitizer a triplet pathway to the photoisomer has been established, the yield of isomer from the triplet state being considerably higher than from direct excitation. On picosecond timescales, two transients are observed; the first has a very short, solvent-independent lifetime, while the second has a longer solvent-dependent lifetime. These two transients are assigned as states formed during the relaxation of the molecules along the first excited singlet and the ground-state potential-energy surfaces, respectively. Similar kinetic behaviour is observed in a high concentration, high viscosity environment designed to mimic the photographic emulsion, indicating that the photo-physical relaxation pathways are still very rapid even in this type of environment.

Pyrazolone and pyrazolotriazole (PT) azomethine dyes are well known as magenta image formers in the photographic subtractive colour development process. They are formed during development by the oxidative coupling of a *p*-phenylenediamine and the appropriate coupler.¹ They exhibit two maxima in their visible absorption spectra; a high intensity band, typically in the green region, and a lower intensity band in the blue region. Unsymmetrical azomethine dyes can exist as two isomeric configurations about the azomethine linkage, referred to as the *syn*- and *anti*-isomers. It has been demonstrated that this isomerisation can be brought about by electronic excitation.² Isomerisation in dyes not symmetrical about the carbon-nitrogen double bond is readily observed as a bathochromic shift in their absorption spectra. The less stable *anti*-isomer so produced relaxes thermally to the *syn*-form on timescales ranging from microseconds to milliseconds depending on temperature, solvent properties and the nature and positions of substituents. Triplet-energy transfer to these dyes also results in production of the isomer, indicating the existence of an isomerisation pathway involving the triplet state. However, the rise of the absorption due to the isomer follows precisely the decay of the sensitizer triplet state irrespective of its lifetime, indicating that the triplet state of the dye must have a lifetime shorter than a few hundred nanoseconds.

Fluorescence quantum yields of these compounds in dilute fluid solution at room temperature are very low,³ of the order of 10^{-4} . Fluorescence quantum yields and fluorescence lifetimes are observed to increase significantly as the temperature is decreased,⁴ although even at liquid nitrogen temperatures no phosphorescence emission can be detected.

Experimental

Solvents were spectrophotometric grade (Aldrich) and were used as received. Dyes were donated by Kodak Ltd. and were used without further purification. The dye structures corresponding to the designations used in the text are shown in Fig. 1. Ultraviolet-visible (UV-VIS) absorption spectra of the dyes in acetonitrile solution are shown in Fig. 2.

The hand coatings are designed to mimic, as far as possible, the photographically formed coatings, but are made with pre-formed dyes and consequently both photographic product dyes and dyes that cannot be formed using the photographic process can be investigated in the product environ-

ment. The formulation of the hand coatings is as follows for a dye with a molecular weight of ca. 1000 g mol^{-1} and a molar absorption coefficient of $10^4 \text{ dm}^3 \text{ mol}^{-1} \text{ cm}^{-1}$, with which parameters an absorbance of approximately 1.5 is obtained at the dye λ_{max} with a dry coating thickness of about $10 \mu\text{m}$. 2.5 g of a 50% gelatin-50% water solid is added to 22.5 g of a 1.39 g dm^{-3} solution of sodium dodecyl sulfate, and the whole heated to dissolve the gelatin. To 20 g of the resulting solution is added a solution of 35 mg of dye and 105 mg of di-*n*-butylphthalate in 2 cm^3 of ethyl acetate, and the whole homogenised using a soniprobe for 5 min. Much of the ethyl acetate evaporates during sonication, and any remaining is removed by additional heating of the mixture prior to proceeding further. The resulting mixture is then spread onto an

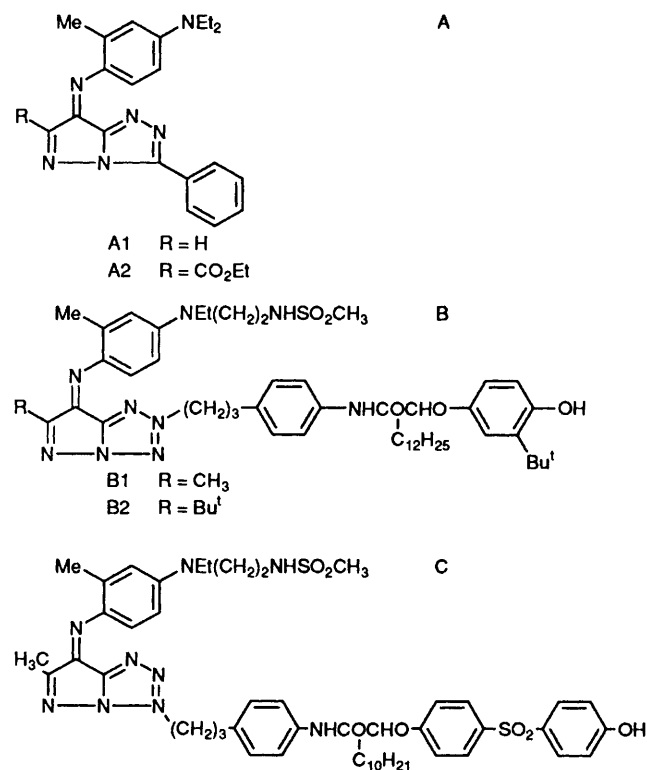


Fig. 1 Pyrazolotriazole azomethine dye structures

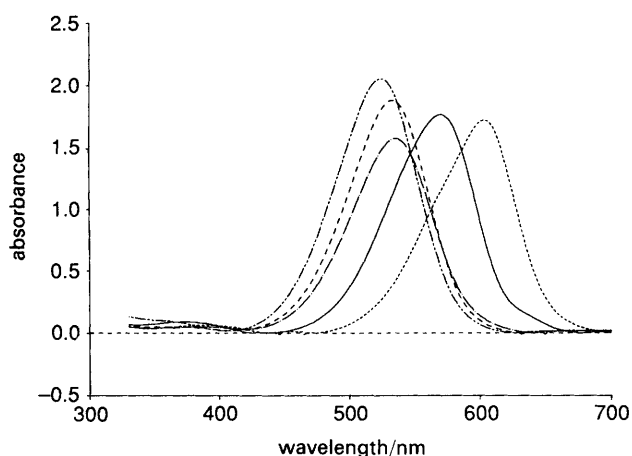


Fig. 2 UV-VIS absorption spectra of pyrazolotriazole azomethine dyes in acetonitrile solution (concentration $4 \times 10^{-5} \text{ mol dm}^{-3}$)

acetate base 'subbed' with gelatin, and dried flat. The mixture is spread at an appropriate thickness given that shrinking of the gelatin causes the dry coating to have a thickness about a tenth that of the wet coating.

Nanosecond laser flash photolysis studies were carried out using an HY200 Nd:YAG laser (Lumonics), frequency doubled to 532 nm for experiments involving direct excitation of the dyes, and frequency tripled to 355 nm for the sensitisation experiments. The analysing source was a 300 W Xenon arc lamp (Optical Radiation Corporation). Detection was with a Hamamatsu R928 photomultiplier tube through an $f/3.4$ grating monochromator (Applied Photophysics). Signals from the photomultiplier tube were digitised with a 2432A digital oscilloscope (Tektronix) and the data transferred to an IBM compatible PC via a GPIB interface for analysis. Opening of shutters for the arc lamp and the laser is computer controlled through a DT2808 D/A interface card (Data Translation). The timing of the system is controlled through a home-built analogue delay generator.

All picosecond experiments were carried out with air equilibrated solutions contained within 1 cm \times 1 cm quartz cuvettes at room temperature (17–21 °C). Nanosecond experiments involving triplet-energy sensitisation were carried out in solutions degassed by three freeze-pump-thaw cycles. Those involving direct excitation of the dye were carried out in air equilibrated solution as oxygen concentration was found to have no effect on the experiments.

Picosecond laser flash photolysis was carried out at the laser support facility at the Rutherford-Appleton laboratory in Oxfordshire. The system consists of an actively mode-locked Nd:YAG laser (Spectron laser systems) synchronously pumping rhodamine 6G in a model 375 B dye laser (Spectra-Physics). The 585 nm output of the dye laser is amplified at 10 Hz in a three-stage dye amplifier pumped by a DCR-3 Q-switched Nd:YAG laser (Quanta-Ray) to a pulse energy in excess of 400 μJ . The amplified beam is split into two, one half being used to provide the excitation pulses while the other is frequency shifted using either stimulated Raman or continuum generation in a water-D₂O mixture to provide the probe pulse, the wavelength of interest being isolated using an interference filter. Excitation pulse energy at the sample was 3–10 μJ per pulse in a 1 mm diameter spot.

The detectors used to monitor the pump and probe signals are based on the design of Pollard and Zenith,⁵ utilising 1 cm \times 1 cm UV sensitive PIN diodes from Hamamatsu (S1723-05). The pump-signal detector is a single diode and amplifier circuit, an integrating sphere being placed in front of the diode to ensure even illumination of the surface. The

probe detector consists of two diodes connected across a differential amplifier circuit, the output from this amplifier being the difference between the two diode outputs, a separate amplification stage providing a signal proportional to the sum of the signals from the two diodes to allow normalisation to probe intensity. The output from each diode is maintained below 250 mV to preserve linearity by the use of appropriate neutral density filters in the probe beam.

The signals from each diode-amplifier combination are fed into SR250 gated integrators (Stanford Research Ltd), which integrate the signals in a gate typically 300 ns wide. The integrated output is then fed to an SR 245 analogue to digital-digital to analogue (A/D D/A) converter and computer interface, and the data fed to a microcomputer via a GPIB interface.

Processing of Pump-Probe Data

The analytical parameter required from these experiments is the change in transmission induced by the pumping pulse at a particular time after its arrival. The normalised probe intensity change induced by the pumping pulse at a time delay t after arrival of the pump pulse of energy P is

$$\left(\frac{\Delta I(P)}{I}\right)_{t,u} = \frac{\bar{D}_{\text{on}} - \bar{D}_{\text{off}}}{\bar{N} - \bar{N}_{\text{baseline}}}$$

where N and D are proportional to the sum and difference signals, respectively, \bar{D}_{on} is the mean difference signal with the pump, \bar{D}_{off} is the mean difference signal with no pump (background signal), $\bar{N}_{\text{baseline}}$ and \bar{N} are the mean sum signal in the absence and presence of incident probe respectively and the subscript u indicates that the value of $\Delta I(P)/I$ is uncorrected and at this stage only proportional to percentage transmission change. No correction for emission is necessary with the samples investigated here since the emission quantum yield at ambient temperatures is too low to be detected. The value of $\Delta I(P)/I$ is then normalised to pump intensity using

$$\left(\frac{\Delta I}{I}\right)_{t,u} = \frac{\left(\frac{\Delta I(P)}{I}\right)_{t,u} \bar{P}_{\text{series}}}{\bar{P} - \bar{P}_{\text{baseline}}}$$

where \bar{P}_{series} is the mean pump intensity for the whole kinetic run. This value of $\Delta I/I$ thus obtained is then corrected to actual percentage transmission change by multiplication by a factor f , obtained from a measurement of the difference signal obtained when an 8% reflecting glass slide is placed in the sample beam. The factor f is then calculated as

$$f = \frac{0.08(\bar{N} - \bar{N}_{\text{baseline}})}{(\bar{D}_{\text{in}} - \bar{D}_{\text{out}})}$$

where \bar{D}_{in} and \bar{D}_{out} relate to the difference signal with the glass slide in and out of the beam, respectively. The analytical parameter most useful in the interpretation of such data, *i.e.* the absorbance change, is calculated from

$$\Delta A = -\log \left[1 - \left(\frac{\Delta I}{I}\right)_i f \right]$$

Results and Discussion

Nanosecond Flash Photolysis

Following flash excitation, population of the *anti*-isomeric form of the dye is observed as a bathochromic shift in the dye absorption spectrum; this shift gives rise to a time-resolved transient difference spectrum as shown in Fig. 3. It is clear

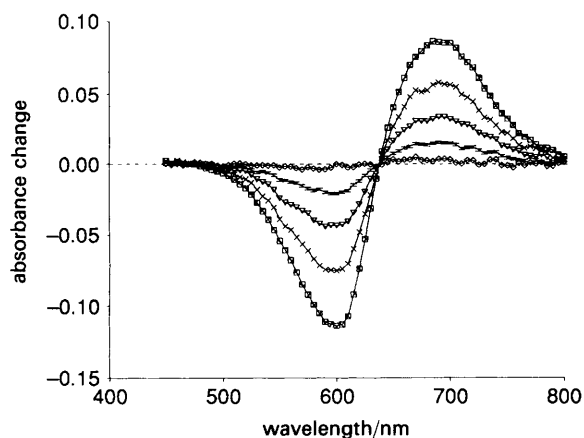


Fig. 3 Transient difference spectrum following pulsed excitation of a 1.68×10^{-5} mol dm^{-3} solution of dye A2 in acetonitrile. Excitation wavelength 532 nm. Time from laser pulse (\square) 0.00066, (\times) 0.00442, (∇) 0.00924, (+) 0.0166 and (\diamond) 0.0319 s.

that the decay kinetics are the same across the entire spectrum.

Quantum Yields of Isomerisation from Singlet and Triplet States

In order to convert the measured photoinduced absorption change due to population of the *anti*-isomer into the quantum yield of isomer production, it is necessary to determine the difference in molar absorption coefficients between the two forms. Assuming no absorption by the *anti*-isomeric form in the short wavelength edge of the *syn*-isomer absorption band the calculated yield is independent of analysis wavelength, and hence the quantum yields presented have been calculated on this basis. The quantum yields of isomer production from direct excitation and from triplet sensitisation are given in Table 1. The triplet-sensitised isomerisation yields are calculated on the basis of a calculated proportion of a known population of sensitising triplet state being quenched by the azomethine dye under investigation, assuming all quenching is by energy transfer.

The same transient difference spectrum is obtained from both triplet-energy sensitisation experiments and as a consequence of direct excitation; this demonstrates that the same product is arrived at by both routes. However, the quantum yield of production of the isomer as a result of direct excitation is substantially less than the yield of isomer from the sensitised triplet state.

Anti-Isomer Relaxation Rates

Once the *anti*-isomer has been populated, either as a result of direct excitation of the dye or by triplet-energy transfer from a suitable donor, it relaxes thermally to the stable *syn*-

Table 1 Isomerisation efficiencies of some pyrazolotriazole azomethine dyes

dye ^a	sensitiser	solvent	<i>anti</i> -isomer quantum yield mean (std. dev.)
A2	none	benzene	0.011 (0.001)
	none	acetonitrile	0.075 (0.006)
	2'-acetonaphthone	benzene	0.4 (0.1)
	benzophenone	benzene	0.4 (0.1)
A1	benzophenone	acetonitrile	0.35 (0.1)
	benzophenone	benzene	0.09 (0.02)
C	benzophenone	benzene	0.45 (0.1)

^a See Fig. 1.

Table 2 *Anti*-isomer relaxation lifetimes

dye	solvent	τ /ms mean (std. dev.)
A2	acetonitrile	7.89 (1.33)
	di- <i>n</i> -butylphthalate	2.13 (0.20)
	methanol	0.279 (0.032)
	benzene	2.22 (0.42)
A1	methanol	452 (4)
	benzene	590 (25)
	chlorobenzene	424 (3)
C	methanol	3.4 (0.5)
	acetonitrile	8.5 (1.5)

configuration by a unimolecular process. The relaxation time is strongly dependent upon both the solvent and the nature of the substituent in the 6-position of the pyrazolotriazole ring of the azomethine dye. Data for the relaxation of *anti*- to *syn*-isomers for a range of substituents and solvents is given in Table 2. All determinations were performed at $21 \pm 1^\circ\text{C}$. Concentrations were in the range $(1.5\text{--}4) \times 10^{-5}$ mol dm^{-3} , and there was no dependence of lifetimes on concentration over the range employed.

Note that there is no correlation between isomer lifetime and bulk solvent properties such as viscosity or relative permittivity; this is illustrated by the relaxation times of the A2 *anti*-isomer in a range of methanol-glycerol mixtures, as shown in Table 3. It is clear that while there is a trend of increasing isomer lifetime with increasing viscosity, this is not the only factor at work, as illustrated by the fact that even with a glycerol : methanol ratio of 20 : 5, and consequently an appreciable viscosity, the isomer lifetime is still shorter than that observed in pure methanol. In addition, no correlation between the *anti*-isomer lifetime and any of the empirical free energy parameters determined for solvents on the basis of equilibria, kinetics and spectroscopic properties⁶ has been found.

The rate of the relaxation process will be determined in part by the free energy of solvation of the transition state through which the interconversion proceeds. Clearly, the group in the *para* position on the aromatic ring attached to the azomethine nitrogen, NEt_2 , is strongly electron donating and as such would be expected to facilitate a torsional mechanism for isomerisation, involving rotation about the carbon-nitrogen double bond, where the negative charge will be delocalised over the pyrazolotriazole ring system.⁹ Therefore a degree of charge separation during the isomerisation process is anticipated to occur, and as such the energy of activation associated with the process may be expected to be lowered in highly polar or polarisable solvents. Inspection of the data of Tables 2 and 3 clearly demonstrates that such a simple relationship between polarity and lifetime does not prevail. However, it is possible that the isomerisation may proceed *via* a biradical intermediate. Indeed, data presented by Douglas and Clarke¹⁰ suggest that A2 may isomerise *via*

Table 3 Dye A2 *anti*-isomer relaxation times in glycerol-methanol mixtures

glycerol : methanol	isomer lifetime/ μs mean (std. dev.)	η/cP^a
pure methanol	279 (32)	0.55
5 : 20	156 (18)	0.88
12 : 13	164 (7)	6.6
20 : 5	174 (12)	133
24 : 1	385 (63)	640

^a Calculated values from ref. 7 and 8.

such a biradicaloid intermediate, this biradical having triplet character assigned on the basis of the pre-exponential factor determined from Arrhenius plots. It is, however, difficult to rationalise the large solvent effects on the thermal back isomerisation rate in A2 on the basis of such a mechanism alone, and the implication therefore is that other processes must be at work in determining the isomer lifetime. For example, it has been noted that the rate of back isomerisation is increased in protic solvents, as a consequence of protonation of the azomethine nitrogen atom,¹¹ which may explain the very large difference in isomer lifetime seen when comparing methanol and acetonitrile solutions where many of the physical solvent properties are similar. It is therefore anticipated that there may be other specific solvent-solute interactions such as this at work in determining the stability of the states involved in any given solvent and hence the rates of *anti-syn*-isomerisation. The thermal back isomerisation rates for dyes A1 and C are much less sensitive to solvent changes than that for A2, which may suggest that a different isomerisation mechanism is dominant in these compounds, possibly one involving less of a change in charge distribution in the transition state relative to the stable conformations, such as inversion over the azomethine nitrogen.

Picosecond Pump-Probe Laser Flash Photolysis

Representative time-resolved transient absorption data are shown in Fig. 4 and 5; these are typical of many more obtained for a range of dye and solvent systems.

General points to note about the kinetic data are:

(a) For all dye and solvent systems it was established that the magnitude of the observed transient absorption was proportional to the exciting laser pulse energy in the range employed (3 to 10 μJ per pulse).

(b) Experiments where the relative polarisation of the pumping and probing beams was changed demonstrated that while the signal recorded with orthogonal polarisations was approximately 2/3 the size of that with parallel polarisations,

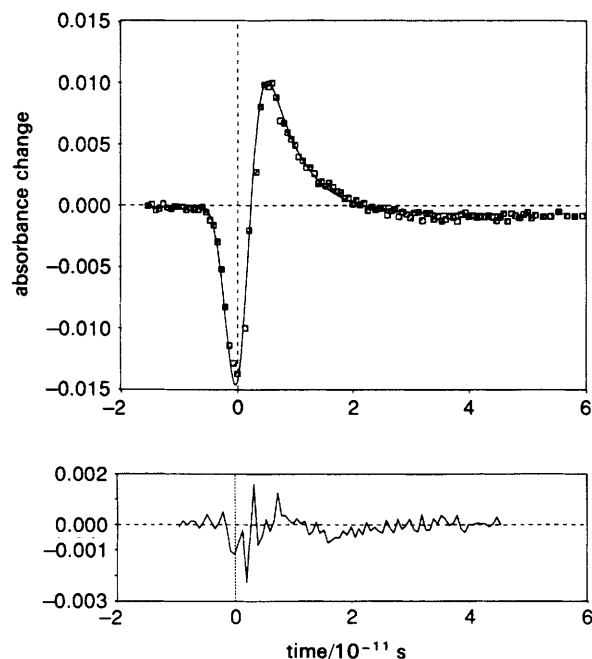


Fig. 4 Picosecond transient absorption trace following excitation of a 7×10^{-6} mol dm^{-3} solution of dye A2 in ethyl acetate. Excitation wavelength 585 nm; analysing wavelength 630 nm; pulse width (FWHM) 3.3 ps. A plot of residuals for the fitted function is also shown.

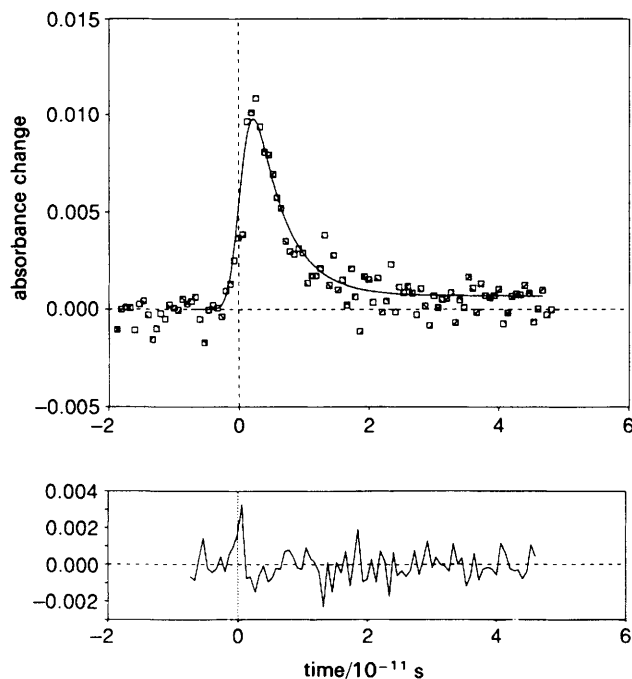


Fig. 5 Picosecond transient absorption trace following excitation of a 4×10^{-5} mol dm^{-3} solution of dye C in toluene solution. Excitation wavelength 585 nm; analysing wavelength 630 nm; pulse width (FWHM) 2.5 ps. A plot of residuals for the fitted function is also shown.

the normalised traces were superimposable. All data presented were recorded with pumping and probing beams oriented at 54.7° to one another to reduce any effects introduced by rotational diffusion.¹²

(c) Measurements of the absorption spectra of the dyes in solution prior to and following the experiments revealed that no detectable sample degradation had occurred, except in the case of dye A2 in the hand coating. Here it was found that the coating suffered damage from laser irradiation, which is attributed to both photochemical degradation and thermal breakdown of the coating structure. As a consequence, in order to record data traces for A2 in the coating, the sample was changed after every five data points, over which period negligible sample degradation occurred.

The kinetic data may be characterised in terms of a biexponential function convolved with a suitable excitation pulse profile; in this instance a Gaussian profile was employed. In order to extract lifetimes as accurately as possible it is necessary to convolute the resulting profile with another Gaussian function describing the probing pulse. The convolution integral¹³ is carried out using Simpson's rule with 13 ordinates. Parameters describing the data can then be extracted and are shown in Table 4. Examples of fits to the data sets are shown in Fig. 4 and 5, with plots of residuals shown for each trace. Some points to note concerning the kinetic data are:

(a) At least two lifetimes are required to fit the data, plus a long-lived component which does not decay on a nanosecond timescale.

(b) The first lifetime is solvent insensitive to within the error of the fitting, the lifetime being 1–3 ps in all solvents. The state associated with this lifetime is not assigned as the Franck-Condon first excited singlet state on the basis of there being no stimulated emission from this state.

(c) The second lifetime shows some solvent dependence, as illustrated in Table 4. However, its lifetime is far too short for it to be assigned as the photoisomer.

Table 4 Best-fit parameters to picosecond data

dye	solvent	λ/nm	ground state		FWHM/ps	τ_1/ps	τ_2/ps	ϵ_1	ϵ_2	ϵ_{isomer}
			ϵ pump	ϵ probe						
A2	MeOH	600	54500	69000	3.7	1.0	6.0	63000	64000	14000
		610	54500	70000	3.3	1.0	4.4	67000	69000	57000
		640	54500	25000	3.4	1.8	3.7	19300	28700	23500
		650	54500	15000	3.5	1.9	5.3	10000	19000	29000
		650	54500	15000	3.5	1.9	5.3	10000	19000	29000
	benzene	640	73000	12000	4.7	2.1	7.4	10000	13200	25000
		650	73000	7000	3.3	1.2	8.9	6000	9200	49000
	DBP	600	67000	83000	3.5	1.0	6.1	82300	79500	27000
		610	67000	15000	2.3	1.0	5.3	85000	85000	86000
		650	67000	8000	3.8	1.0	7.7	13500	17000	30000
	MeCN	630	40000	25000	3.5	0.7	8.7	17000	27000	24000
		640	40000	30600	3.6	0.5	9.6	8000	16000	15000
		650	40000	17000	3.3	0.6	10.1	2600	11000	10000
		650	40000	17000	3.3	0.6	10.1	2600	11000	10000
	hexane	630	7000	300	1.0	0.9	6.7	750	2700	8000
EtOAc	630	45000	23500	3.1	1.0	5.8	20000	26000	22500	
coating	640	65000	17000	4.5	5.3	6.3	15000	35000	31000	
B1	toluene	650	3500	200	2.3	0.8	2.1	330	1000	9000
B2	toluene	650	3500	200	2.4	1.0	2.6	360	1200	3000
C	toluene	630	7000	725	2.5	0.5	4.7	800	2000	3500
		640	7000	425	2.5	0.9	4.7	800	2000	3500
		650	7000	200	3.0	0.7	3.7	440	500	1000

FWHM pulse full-width-half-maximum, λ probe wavelength, MeOH methanol, MeCN acetonitrile, EtOAc ethyl acetate, DBP di-*n*-butylphthalate, ϵ values quoted have units of $\text{dm}^3 \text{mol}^{-1} \text{cm}^{-1}$.

(d) The long-lived component necessary to fit the data has identical spectral properties to the photoisomer observed following pulsed excitation on nanosecond timescales. The molar absorption coefficient of this state presented in Table 4 is calculated using isomerisation quantum yields determined from nanosecond flash photolysis experiments. In all cases this component shows no decay on the timescale accessible with the picosecond apparatus, and is consequently assigned as the photoisomer.

Therefore we propose a model for the *syn-anti*-photoisomerisation process whereby the assignment of the states associated with lifetimes τ_1 and τ_2 are as shown in Fig. 6.

First Short-lived Transient associated with Lifetime τ_1

The kinetic traces obtained for dye A2 probing between 600 and 650 nm in all solvents (except hexane where the *syn*-isomer absorption spectrum is hypsochromically shifted) show an initial prompt bleaching which recovers in 0.5–3 ps. The data for dyes C, B1, and B2 do not show any initial bleaching by virtue of the very small absorption by the *syn*-isomer ground state in the probed spectral region. Since there is no evidence for stimulated emission from this state, it is not assigned as the fluorescent singlet state. There then remains the possibility that it is in fact the twisted excited

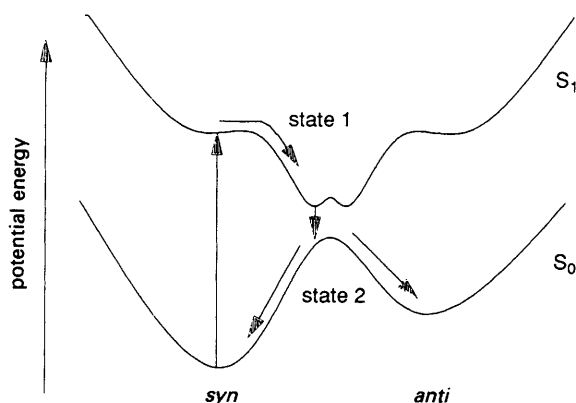


Fig. 6 Schematic potential-energy surface for the pyrazolotrazole azomethine dyes

singlet state at the perpendicular conformation. Within experimental error, the lifetime of this state shows little solvent dependence, although there is evidence that it is slightly longer lived when the environment is that of the dye-di-*n*-butylphthalate droplet in the hand coating than in fluid di-*n*-butylphthalate solution. Changes in lifetime with solvent would, however, be very difficult to detect because of the coupling between the lifetime of this state, its molar absorption coefficient and the pulse width. It is proposed therefore that excitation takes place initially to the first excited singlet state of the *syn*-isomer, and it is this which is the fluorescent singlet state. However, at the temperatures and low viscosities used throughout this work this state is very short-lived and the population immediately evolves toward the perpendicular conformation. As a consequence, the steady-state population of the fluorescent singlet state is very small, explaining the lack of stimulated emission. Hence what is termed here for simplicity as 'state 1' could in fact be thought of as being the excited-state population as it evolves toward the perpendicular conformation, and will therefore have an 'effective absorption coefficient' which varies with time since the absorption coefficient will undoubtedly vary somewhat with position on the excited singlet state surface. Evolution to the perpendicular conformation is therefore postulated as very rapid, the rate-limiting step in reaching the ground-state surface in fluid solution being internal conversion from the perpendicular conformation. This may be relatively insensitive to solvent parameters provided the ground to excited state surface separation does not significantly change with changing solvent. Such changes may be expected to occur if there were significant charge separation in the perpendicular geometry, and hence the suggestion is tentatively made that this is not the case and that isomerisation proceeds possibly *via* homolytic fission of the azomethine bond to yield the singlet biradical, followed by torsion about this bond. In the hand coating, the state 1 lifetime is seen to be longer than in fluid solution, and here evolution of the population to the twisted geometry is postulated as rate determining.

Second, Longer-lived Transient associated with Lifetime τ_2

Again taking the example of the data obtained with A2 first, it can be seen from inspection of data in Table 4 that the

Table 5 State 2 lifetime as a function of solvent

solvent	τ /ps mean (std. dev.)
methanol	4.4 (0.9)
di- <i>n</i> -butylphthalate	6.3 (1.1)
benzene	8.1 (1.0)
acetonitrile	9.5 (0.7)

absorption coefficient of this state is somewhat less than that of the *syn*-isomer ground state at wavelengths shorter than 630 nm, but somewhat greater at longer wavelengths. The lifetime of the state also exhibits some solvent dependence, the mean lifetimes as a function of solvent being shown in Table 5.

Again, there is no correlation between lifetime and either solvent relative permittivity or viscosity. Interestingly, however, the increase of state 2 lifetime with solvent follows the same pattern as that of the lifetime of the *anti*-isomer (Table 2). This lends weight to the theory which naturally follows from the assignment of state 1 that state 2 is a point (or points) on the ground-state potential surface. The transient seen as state 2 may then be assigned as the evolution of the population along the ground-state surface returning to equilibrium, and again there will be some position dependence of the absorption coefficient on this surface and the transient seen will reflect the population in the ground-state evolving toward the two isomeric forms. The precise reasons why there is no clear correlation between solvent properties and the measured state 2 lifetimes are not known, although several theories have been advanced for the lack of correlation of isomerisation rates in, for example, stilbenes with solvent viscosity.¹⁴ These may be summarised as:

(i) The intramolecular potential surfaces exhibit a solvent dependence (specific solvent-solute interactions).

(ii) Macroscopic solvent viscosity is not an adequate measure of the friction felt by the isomerising molecule, possibly as a consequence of the molecular scale involved in the isomerisation process.

(iii) Other degrees of freedom than the isomerisation coordinate may contribute to the overall relaxation process.

It is felt that, given the complexity of the dyes involved, probably all of the above make some contribution to the overall explanation, although given the small size of the moiety involved in the isomerisation process one may expect the failure of the macroscopic viscosity to describe adequately the prevailing friction to play a major role. The data collected for dyes B1 and B2 in toluene solution demonstrate that these two dyes exhibit identical properties (Table 4). This suggests that steric hindrance in the 6-position is not an important factor in determining the state 2 lifetime.

It should be pointed out at this juncture that there is no direct evidence from the data that state 1 is a precursor of state 2, and there exists the possibility that both states form simultaneously; the data are then simply the superposition of two transients. However, it is simpler to rationalise the observed transients on the basis of a sequential model, so in the absence of evidence to the contrary such a model will be adopted.

Conclusions

The two picosecond transients observed have been assigned as states 1 and 2 which may be represented as in Fig. 6. State 1 is evolution of the excited-state population to the twisted excited-state conformation, which may have a short but finite

lifetime; on the basis of the quantum yields of isomer formation (Table 1), a potential minimum on the excited state surface is postulated to be located on the *syn*-isomer side of the potential barrier between *syn*- and *anti*-isomeric forms. This assignment is favoured on account of the lack of stimulated emission observed, which can be explained if the population of the initially formed fluorescent state is vanishingly small. This is suggested to be a consequence of a very small potential barrier from the initially formed state and a very steep potential toward the perpendicular conformation. Such very fast decay times and lack of solvent dependence have been observed for the photoisomerisation of *cis*-stilbene, and this has also been explained as resulting from the presence of a very small activation barrier in the excited state. However, following internal conversion to the ground-state potential surface the molar absorption coefficient thereof is not observed to change significantly with time.¹⁵ In the case of the azomethine dyes, state 2 is assigned as the population on the ground-state surface evolving to the two isomeric forms, the absorption coefficient varying with position on the surface. The frequency of the motion on the ground-state surface shows some solvent dependence, and this is the same dependence as seen for the thermal *anti*-*syn*-isomerisation following population of the *anti*-isomer. This picture was suggested by us as a possible explanation in a preliminary publication on this work¹⁶ prior to gathering much of this data. Following this earlier publication, data presented by Douglas *et al.*⁴ have been rationalised in terms of a similar picture. These authors succeeded in detecting the fluorescent singlet state of A2 in a 96 : 4 v/v glycerol : methanol mixture at room temperature from stimulated emission measurements, this state having a lifetime of ≤ 2 ps. However, they could not detect such a state in pure ethanol solution, results which are in agreement with those presented here.

The authors wish to thank Kodak Ltd. for kindly supplying the dyes used, and SERC for financial support.

References

- 1 T. H. James, in *The Theory of the Photographic Process*, Macmillan, London, 4th edn., 1988.
- 2 W. G. Herkstroeter, *J. Am. Chem. Soc.*, 1976, **95**, 330.
- 3 P. Douglas, *J. Photogr. Sci.*, 1988, **36**, 83.
- 4 P. Douglas, S. M. Townsend, R. J. Booth, B. Crystall, J. R. Durrant and D. R. Klug, *J. Chem. Soc., Faraday Trans.*, 1991, **87**, 3479.
- 5 H. J. Pollard and W. Zenith, *J. Phys. E*, 1985, **18**, 399.
- 6 C. Reichardt, in *Solvents and Solvent Effects in Organic Chemistry*, VCH, Weinheim, 2nd edn., 1988.
- 7 *Perry's Chemical Engineers Handbook*, ed. D. W. Green, McGraw-Hill, New York, 6th edn., 1984.
- 8 *Physical Properties of Binary Systems in Concentrated Solutions*, ed. J. Timmermans, Interscience, New York, 1959, vol. 2.
- 9 H. Kessler, *Angew. Chem.*, 1970, **82**, 237.
- 10 P. Douglas and D. Clarke, *J. Chem. Soc., Perkin Trans. 2*, 1991, 1363.
- 11 C. Couture and P. Douglas, Poster abstract No. II-71, XVth International Conference on Photochemistry, Paris, France, 1991.
- 12 H. E. Lessing and A. von Jena, *Chem. Phys. Lett.*, 1976, **42**, 213.
- 13 D. F. Eaton, *Pure Appl. Chem.*, 1990, **62**, 1631.
- 14 S. K. Kim and G. R. Fleming, *J. Phys. Chem.*, 1988, **92**, 2168.
- 15 S. Abrash, R. Repinec and R. M. Hochstrasser, *J. Chem. Phys.*, 1990, **93**, 1041.
- 16 F. Wilkinson, D. R. Worrall and R. S. Chittock, *Chem. Phys. Lett.*, 1990, **174**, 416.